Available online at www.sciencedirect.com

ScienceDirect

Ceramics International 39 (2013) 9743–9747

CERAMICS INTERNATIONAL

www.elsevier.com/locate/ceramint

Short communication

Indentation response of pulsed electric current sintered polymer derived HfO_2/Si–C–N(O) nanocomposites

Ravindran Sujith, Ravi Kumar*

Materials Processing Section, Department of Metallurgical and Materials Engineering, Indian Institute of Technology Madras, Chennai 600036, India

Received 27 February 2013; received in revised form 22 April 2013; accepted 28 April 2013
Available online 4 May 2013

Abstract

The influence of pulsed electric current sintering on the structural evolution and indentation response of hafnia incorporated silicon carbonitride polymer derived ceramics was studied. Despite the absence of any sintering additives, appreciable sintering at 1400 °C with a density of ~2.7 g/cc was observed. Sintering beyond 1300 °C resulted in the phase separation and nano-crystallization of amorphous Si–Hf–C–N–O ceramic. The crystallite coarsening was insignificant and thereby the tetragonal phase of hafnia was retained in the ceramic nanocomposite. A relatively high indentation hardness and elastic modulus of ~18 GPa and ~313 GPa were determined by depth sensing nanoindentation technique.

Keywords: A. Precursors: organic; A. Sintering; B. Nanocomposites; C. Mechanical properties

1. Introduction

The development of transition metal oxide incorporated polymer derived ceramics (PDC) has gained immense interest in recent times [1–6]. In contrast to ternary Si- based PDCs such as Si–O–C and Si–C–N ceramics, specific improvement in the material properties can be achieved by the chemical modification of these ceramics by the incorporation of various transition metal oxides such as titania [2], zirconia [4] and hafnia [5,6]. Among these transition metal oxides, hafnia incorporated Si based ceramic nanocomposites are of special interest because of its technological potential, for instance, in microelectronics industry [7]. However, the existing literature is restricted to the synthesis, structural evolution and thermal stability of HfO_2/Si–C–N(O) ceramic nanocomposites. [5,6,8–12]. The potential of these nanocomposites for possible structural applications necessitates a need to comprehensively understand the mechanical behavior which was not explored till date.

The present study focuses on the evaluation of the indentation response of HfO_2/Si–C–N(O) ceramic nanocomposites produced by pulsed electric current sintering (PECS). PECS was adopted for the production of dense transition metal oxide incorporated PDCs for the first time. The technique serves as a unique and efficient sintering tool due to the possibility of attaining high densification rates. Upon sintering, significant densification was observed for the HfO_2/Si–C–N(O) ceramic nanocomposites, unlike the unmodified Si–C–N ceramics. Remarkably, tetragonal hafnia phase was retained as a stable phase even after sintering at a temperature of 1500 °C. This could be of potential interest in the development of materials with high dielectric properties, due to higher dielectric constant associated with the tetragonal phase in contrast to the monoclinic phase [7]. The hardness and elastic modulus determined for these HfO_2/Si–C–N(O) ceramic nanocomposites were also among the highest reported for any ceramics produced by the precursor route.

2. Experimental

Hafnium modified polysilazane was synthesized by the chemical modification of polysilazane (HTT1800, Clariant, Germany). The polysilazane was modified by the addition of 30 vol% hafnium tetra n-butoxide (Sigma-Aldrich, India) and stirred for about 30 min in Ar atmosphere. The modified

*Corresponding author. Tel./fax: +91 44 22574777.
E-mail address: nvrk@iitm.ac.in (R. Kumar).

0272-8842/$ - see front matter © 2013 Elsevier Ltd and Techna Group S.r.l. All rights reserved.
http://dx.doi.org/10.1016/j.ceramint.2013.04.095

polysilazane was crosslinked at 300 °C for 3 h and subsequently thermolysed in Ar atmosphere at 1300 °C for 2 h at a constant heating rate of 5 °C/min [11]. The as-thermolysed powder was ground and powder of particle size less than 125 μm was chosen for PECS (Sumitomo Coal Mining Co. Ltd., Japan). The sintering was performed in vacuum at 1300, 1400 and 1500 °C and the sintered ceramic compacts hereafter will be referred to as SiHfCNO1300, SiHfCNO1400 and SiHfCNO1500, respectively. The pressure, holding time and heating rate were maintained constant at 30 MPa, 30 min and 50 °C/min, respectively. For sintering, a pulse ratio of 12/2 ms on/off was chosen. For comparison, unmodified Si–C–N ceramic powder produced by the thermolysis of polysilazane at 1300 °C in Ar atmosphere was sintered and will be hereafter referred as SiCN1500.

The microstructure of the PECS ceramics was observed by field emission scanning electron microscopy (FE-SEM) using FEI Quanta 400, USA. The elemental composition was obtained from the energy dispersive X-ray spectroscopy (EDX) using scanning electron microscopy (FEI Quanta 200, USA). The apparent density of these ceramics was determined by water displacement method. Furthermore the open porosity (%) was calculated as per Eq. (1) [13].

$$p(\%) = (m_w - m_d)/(m_w - m_{ww}) \quad (1)$$

where, m_w is the weight of the wet sample (g), m_d is the weight of the sample (g) and m_{ww} is the weight of the sample immersed in water (g). The structural evolution upon sintering was understood from X-ray diffraction (D8 Discover, Bruker AXS X-ray Diffractometer, USA) using Cu K_α radiation ($\lambda = 0.15408$ nm) in the 2θ range of 5–90°. The crystallite sizes were determined using the Scherrer equation. The hardness and elastic modulus were measured by depth sensing nanoindentation technique (Hysitron Inc., USA). A standard Berkovich indenter was used and the area function was calibrated by performing a set of 25 indents on fused quartz. For nanoindentation, all the samples were polished as per standard ceramographic practice. The indentations were performed at a maximum load (P_{max}) of 10 mN. A trapezoidal loading function was used maintaining a constant loading rate of 1 mN/s, holding time of 10 s and unloading rate of 1 mN/s. Further, micro-Vickers indentation (Wolpert Wilson 4325VA, USA) was performed at a maximum load of 9.81 N and for a holding time of 10 s. The Poisson's ratio of the samples was determined by non-destructive resonant frequency testing method.

3. Results and discussion

Fig. 1 shows the variation in displacement rate with time for SiHfCNO1300, SiHfCNO1400, SiHfCNO1500 and SiCN1500 ceramics. A representative sintering temperature profile at 1500 °C is shown. From the figure it can be inferred that the sintering is insignificant until 1300 °C and is maximum beyond 1400 °C deducing that densification of these highly covalent bonded ceramics at temperature below 1300 °C was difficult. Moreover, SEM images of SiCN1300 and SiHfCNO1300 also

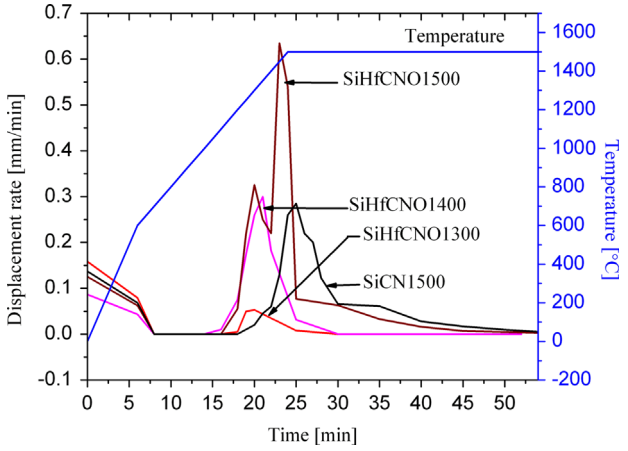

Fig. 1. Variation in densification rate with temperature during PECS for SiCN1500, SiHfCNO1300, SiHfCNO1400 and SiHfCNO1500. A representative temperature profile of PECS at 1500 °C is also shown.

reveals to this and are depicted in Fig. 2(a) and (b). A representative micrograph of the sintered Si–Hf–C–N–O (SiHfCNO1500) and its magnified image are shown in Fig. 2(c) and (d) respectively. The bright regions correspond to the hafnium rich regions inferring localized variation in hafnium content (see Fig. 2d). Similar microstructural features were reported in the literature for the Si–Hf–C–N–O ceramics obtained from the same polymeric precursor (HTT1800) [11]. In addition, the sintering of Si–Hf–C–N–O ceramics seems to begin early in contrast to Si–C–N ceramics. For instance, sintering started at the 20th min for Si–Hf–C–N–O ceramics, in contrast to a couple of minutes later for Si–C–N suggesting better sinterability of the former (Fig. 1).

The apparent density of SiHfCNO1300, SiHfCNO1400 and SiHfCNO1500 were ~2.04, 2.74 and 2.85 g/cc, respectively while the density of SiCN1500 was ~2.07 g/cc. Moreover, the extent of open porosity in these ceramics was significantly reduced from ~19% (SiHfCNO1300) to ~4% (SiHfCNO1500) with the increase in sintering temperature inferring substantial densification of the latter (Table 1). The higher densification achieved for Si–Hf–C–N–O ceramics can possibly be attributed to the presence of Si–O bonds in the Si–C–N(O) matrix which may enhance the solid state diffusion capability of the material. The reaction pathway suggested in the literature reported for the synthesis of hafnium modified Si–C–N(O) ceramic establishes the presence of Si–O bonds in the hafnium alkoxide modified polysilazane [11]. Furthermore, it should be noted that the phase separated HfO_2 due to its ionic nature could have also contributed to the enhanced solid state sinterability [14].

From Fig. 3 it is inferred that the as-thermolysed Si–Hf–C–N–O ceramic is X-ray amorphous. Upon PECS, SiHfCNO1300 retained its amorphous nature in contrast to SiHfCNO1400 and SiHfCNO1500 which exhibited phase separation and crystallization resulting in the formation of HfO_2/Si–C–N(O) ceramic nanocomposites. The high intensity peaks at $2\theta = 30.1$, 35.1, 50.3 and 59.7° were assigned to tetragonal hafnia and the relatively low intense peak at $2\theta = 28.3°$ was assigned to monoclinic hafnia (Fig. 3). In addition, a peak at $2\theta = 26°$ was observed and was

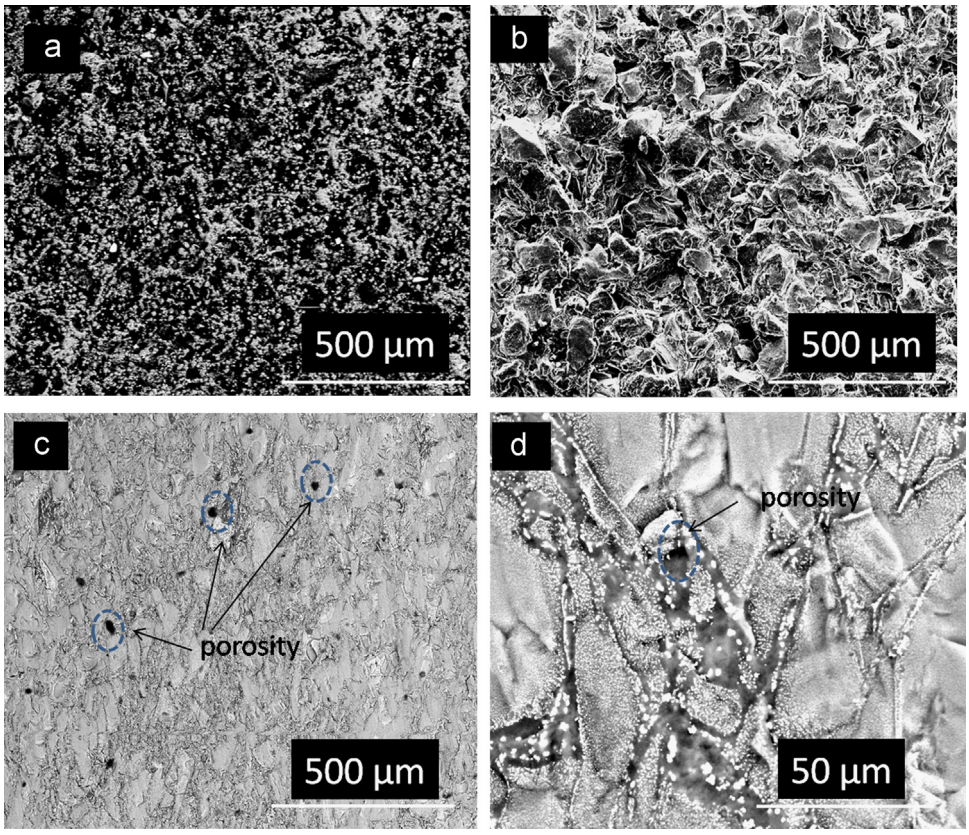

Fig. 2. Backscattered electron micrographs of (a) unsintered Si–C–N (SiCN1500), (b) unsintered Si–Hf–C–N–O (SiHfCNO1300), (c) sintered Si–Hf–C–N–O (SiHfCNO1500) and (d) magnified backscattered image of SiHfCNO1500 (bright regions indicate localized enrichment of hafnium).

Table 1
Elemental composition and open porosity of PECS Si–C–N and Si–Hf–C–N–O.

Material system	Si (wt%)	Hf (wt%)	C (wt%)	N (wt%)	O (wt%)	Porosity (%)
SiCN1500	~26	–	~68	~3	~3	13.9
SiHfCNO1300	~45	~13	~20	~9	~13	18.8
SiHfCNO1400	~42	~17	~24	~9	~8	9.3
SiHfCNO1500	~46	~16	~21	~9	~8	4.2

assigned to the presence of excess free carbon which is in agreement with the literature [15]. The crystallite sizes of tetragonal hafnia for SiHfCNO1400 and SiHfCNO1500 were ~14 and ~16 nm respectively, inferring insignificant coarsening. The stability of tetragonal hafnia phase at room temperature was attributed to the crystallite size effect. In a previous study we reported that below a critical crystallite radius of ~4 nm, hafnia can exist only as a tetragonal phase [8]. However, with coarsening the tetragonal phase becomes unstable and transforms to a monoclinic phase, which is the room temperature stable phase of hafnia. This suggests that the coarsening has a significant role to play as far as the stability of the tetragonal phase of hafnia is concerned. However, due to the extremely low diffusion time scales associated with PECS, coarsening was considerably restricted aiding retention of the tetragonal crystal structure. Moreover, it is interesting to notice that under similar processing conditions SiCN1500 phase separated and crystallized, which is evident by the presence of β-SiC as exemplified from the XRD (Fig. 3). The absence of Si_3N_4 in the XRD suggests the unstable nature of Si_3N_4 in vacuum beyond 1300 °C. Upon sintering beyond 1300 °C a substantial drop in the vacuum pressure was observed for the unmodified Si–C–N ceramic. The thermodynamic calculations performed earlier on Si–C–N indicated that at low N_2 partial pressures the decomposition of Si_3N_4 to nitrogen gas and liquid or solid silicon could occur as early as 1300 °C [16]. A similar trend in the sintering behavior was reported for the PECS of Si–C–N with yttria as an additive [17]. However, the equivalent carbo-thermal decomposition was not observed in the case of Si–Hf–C–N–O ceramics. This could be also inferred from the elemental composition wherein the weight (%) remained similar for SiHfCNO1400 and SiHfCNO1500 (Table 1). These results suggest the possible influence of hafnia nanocrystallites on the stabilization of Si–C–N(O) matrix preventing further thermal decomposition. A similar inference was reported for the zirconia modified Si–O–C ceramic [4].

An exemplary illustration of the load-displacement curves of SiCN1500, SiHfCNO1300, SiHfCNO1400 and SiHfCNO1500 are shown in Fig. 4. From the load-displacement curves, the hardness and the reduced elastic modulus (E_r) were determined by the Oliver–Pharr method [18]. The validity of this method for the determination of hardness and elastic modulus was ensured by determining the elastic work ratio. The elastic work ratio is defined as the ratio of the work done in the elastic part

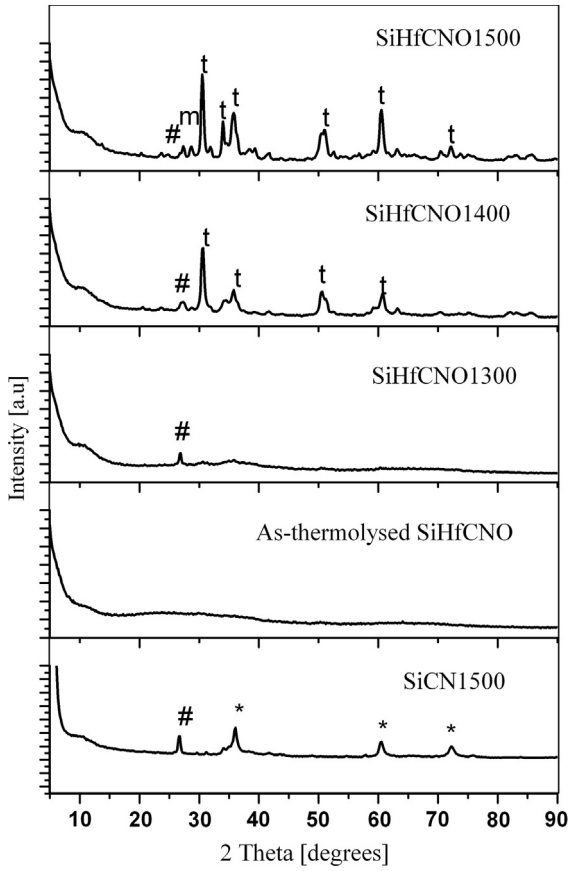

Fig. 3. XRD showing the structural evolution upon PECS of SiCN1500, as-thermolysed SiHfCNO, SiHfCNO1300, SiHfCNO1400 and SiHfCNO1500 (t—tetragonal HfO_2, m—monoclinic HfO_2, ♯—graphite, ∗—β SiC).

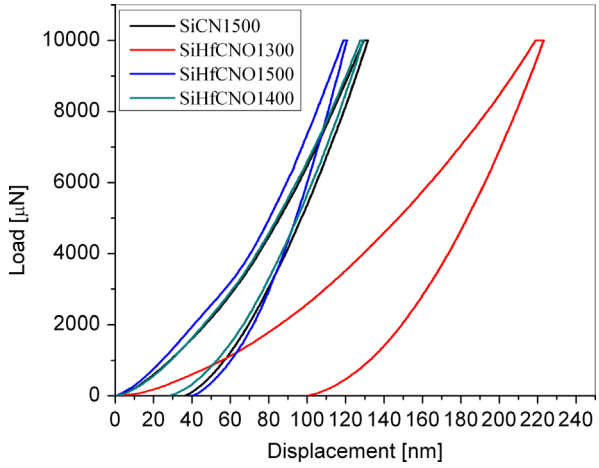

Fig. 4. Representative load-displacement curves for SiHfCNO1400, SiHfCNO1500 and fused quartz.

of the deformation (W_{el}) to the total work done (W_{tot}). It is observed that for materials with low elastic work ratio, typically less than 0.5, the calculated hardness overestimate due to the significant contribution from the pile-ups [19]. The elastic work ratio for SiHfCNO1400 and for SiHfCNO1500 were estimated to be ~0.73 and ~0.65, respectively.

The reduced elastic modulus determined from nanoindentation is given by the following expression.

$$1/E_r = (1-\nu^2)/E + (1-\nu_i^2)/E_i \quad (2)$$

where, E and E_i are the elastic modulii of the sample and the diamond Berkovich indenter respectively and ν and ν_i are their respective Poisson's ratios. E and ν for the samples are provided in Table 2, whereas, E_i and ν_i are taken as 1140 GPa and 0.07, respectively. Table 2 provides the indentation hardness and elastic modulus for SiCN1500, SiHfCNO1300, SiHfCNO1400 and SiHfCNO1500. The hardness and elastic modulus values of SiCN1500 were ~15 GPa and ~196 GPa respectively. The hardness value was in close agreement with that of Si–C–N ceramic produced by the cast route [20,21], whereas the elastic modulus was ~40% higher for the PECS Si–C–N, possibly due to the rigid structure obtained by the PECS technique. However, for Si–Hf–C–N–O ceramics, with increase in sintering temperature from 1300 to 1500 °C, the elastic modulus was increased by ~85%. Similar behavior of increase in elastic modulus with progressive increase in sintering temperature was reported in the literature [21]. An equivalent increase in the hardness value (~20%) was also observed for SiHfCNO1300 through SiHfCNO1400 (Table 2). It should be noted that SiHfCNO1300 was X-ray amorphous having weak Si–O–Hf bond in the ceramic network [11]. While SiHfCNO1400 was phase separated and existed in the form of HfO_2/Si–C–N(O) ceramic nanocomposite. The progressive removal of Hf–O bond from the initial ceramic network would have contributed to the increased network rigidity and resistance to deformation resulting in higher hardness and elastic modulus values for SiHfCNO1400. However, with further increase in sintering temperature to 1500 °C no further densification (Table 2) or change in elemental composition was observed (Table 1). This could have attributed to the similar hardness values for SiHfCNO1400 and SiHfCNO1500. The hardness determined by micro-Vickers indentation for SiHfCNO1400 and SiHfCNO1500 were also observed to be constant of ~16 GPa (Table 2). However, micro-indentation experiments were not carried out for SiCN1500 and SiHfCNO1300 because of the practical difficulty to locate pore-free location.

4. Conclusions

In the current study, PECS was adopted for the production of SiHfCNO ceramics. The density, hardness and elastic modulus of these ceramics were found to be among the highest reported in the literature. The amorphous SiHfCNO1300 ceramic showed no appreciable sintering, whereas the phase separated and crystallized ceramics sintered at 1400 and 1500 °C showed significant densification. As a result of the short processing time scales involved in the PECS and slow bulk diffusion rates due to the covalent bonded Si–C–N(O) matrix, the crystallite growth of hafnia was insignificant. Hence, the production of near dense HfO_2/Si–C–N(O) nanocomposites with retained tetragonal hafnia

Table 2
Material properties of fused quartz, SiCN1500, SiHfCNO1300, SiHfCNO1400 and SiHfCNO1500.

Material system	Density (g/cc)	Poisson's ratio	Nanoindentation hardness (GPa)	Elastic modulus (GPa)	Micro-Vickers hardness (GPa)
Fused quartz	2.20	0.17	8.15 ± 0.20	67 ± 1	*
SiCN1500	2.07	*	15.01 ± 0.17	196 ± 4	*
SiHfCNO1300	2.05	*	13.28 ± 1.15	161 ± 12	*
SiHfCNO1400	2.74	0.25	18.20 ± 0.50	218 ± 3	16.40 ± 1.30
SiHfCNO1500	2.85	0.23	18.20 ± 0.60	313 ± 14	15.30 ± 2.70

*—Not determined due to porosity.

phase microstructure could be of potential technological importance.

Acknowledgments

We are thankful to the Center for Non-destructive Evaluation (CNDE)—Indian Institute of Technology Madras for providing access to resonance frequency testing. The technical assistances received from Mr. N. S. Karthiselva and Mr. Devinder Yadav for the operation of FE-SEM at Indian Institute of Technology Madras is also gratefully acknowledged.

References

[1] R. Hauser, A. Francis, R. Theismann, R. Riedel, Processing and magnetic properties of metal-containing SiCN ceramic micro- and nano-composites, Journal of Materials Research 18 (2003) 2549–2551.
[2] K. Sato, T. Saitoh, T. Nagano, Y. Iwamoto, Low temperature crystallization behavior of α-Si_3N_4 from Ti-doped amorphous silicon nitride derived from polytitanasilazanes, Journal of Ceramic Society Japan 114 (2006) 502–506.
[3] E. Xie, S. Cao, J. Wang, X. Yan, S. Bernard, P. Miele, Engineering of silicon- based ceramic fibers: novel SiTaC(O) ceramic fibers prepared from polytantalosilane, Materials Science and Engineering A 527 (2010) 7086–7091.
[4] E. Ionescu, C. Linck, C. Fasel, M. Muller, H.J. Kleebe, R. Riedel, Polymer- derived SiOC/ZrO_2 ceramic nanocomposites with excellent high temperature stability, Journal of the American Ceramic Society 93 (2010) 241–250.
[5] E. Ionescu, B. Papendorf, H.J. Kleebe, F. Poli, K. Muller, R. Riedel, Polymer- derived silicon oxycarbide/hafnia ceramic nanocomposites. Part I: phase and microstructure evolution during the ceramization process, Journal of the American Ceramic Society 93 (2010) 1774–1782.
[6] E. Ionescu, B. Papendorf, H.J. Kleebe, R. Riedel, Polymer- derived silicon oxycarbide/hafnia ceramic nanocomposites. Part II: stability toward decomposition and microstructure, Journal of the American Ceramic Society 93 (2010) 1783–1789.
[7] X. Zhao, D. Vanderbilt, First-principles study of structural, vibrational, and lattice dielectric properties of hafnium oxide, Physical Review B 65 (2002) 1–4 233106.
[8] R. Sujith, A.B. Kousaalya, R. Kumar, Coarsening induced phase transformation of hafnia in polymer- derived Si–Hf–C–N–O ceramics, Journal of the American Ceramic Society 94 (2011) 2788–2791.
[9] R. Sujith, A.B. Kousaalya, R. Kumar, Synthesis and phase stability of precursor derived HfO_2/Si–C–N–O nanocomposites, Ceramic International 38 (2012) 1227–1233.
[10] S. Brahmandam, R. Raj, Novel composites constituted from hafnia and a polymer derived ceramic as an interface: phase for severe ultrahigh temperature applications, Journal of the American Ceramic Society 90 (2010) 3171–3176.
[11] B. Papendorf, K. Nonnenmacher, E. Ionescu, H.J. Kleebe, R. Riedel, Strong influence of polymer architecture on the microstructural evolution of hafnium alkoxide modified silazanes upon ceramization, Small 7 (2011) 970–978.
[12] H.J. Kleebe, K. Nonnenmacher, E. Ionescu, R. Riedel, Decomposition-coarsening model of SiOC/HfO_2 ceramic nanocomposites upon isothermal anneal at 1300 °C, Journal of the American Ceramic Society 95 (2012) 2290–2297.
[13] E. Ionescu, C. Linck, C. Fasel, M. Müller, H.-J. Kleebe, R. Riedel, Polymer-derived SiOC–ZrO_2 ceramic nanocomposites with excellent high-temperature stability, Journal of the American Ceramic Society 93 (2010) 241–250.
[14] P. Babilo, S.M. Haile, Enhanced sintering of ytrrium doped barium zirconate by addition of ZnO, Journal of the American Ceramic Society 88 (2005) 2362–2368.
[15] M. Esfehanian, R. Oberacker, T. Fett, M.J. Hoffmann, Development of dense filler-free polymer-derived SiOC ceramics by field-assisted sintering, Journal of the American Ceramic Society 91 (2008) 3803–3805.
[16] J. Peng, Thermochemistry and Constitution of Precursor Derived Si–(B–) C–N Ceramics, 1–139 Ph.D. Thesis.
[17] J. Wan, M.J. Gasch, A.K. Mukherjee, Silicon nitride–silicon carbide nanocomposites fabricated by electric-field-assisted sintering, Journal of the American Ceramic Society 86 (2002) 526–528.
[18] W.C. Oliver, G.M. Pharr, An improved technique for determining hardness and elastic modulus using load and displacement sensing indentation experiments, Journal of Materials Research 7 (1992) 1564–1583.
[19] M. Rodríguez, J.M. Molina-Aldareguía, C. Gonzalez, J. LLorca, Determination of the mechanical properties of amorphous materials through instrumented nanoindentation, Acta Materialia 60 (2012) 3953–3964.
[20] N. Janakiraman, F. Aldinger, Fabrication and characterization of fully dense Si–C–N Ceramics from a poly(ureamethylvinyl)silazanes precursor, Journal of the European Ceramic Society 29 (2009) 163–173.
[21] N. Janakiraman, F. Aldinger, Indentation analysis of elastic and plastic deformation of precursor-derived Si–C–N ceramics, Journal of the European Ceramic Society 30 (2010) 775–785.